BELLCOMM, INC.

TR-66-340-1

Model Distribution of Photographic Meteors

March 29, 1966

J. S. Dohnanyi

Work performed for Manned Space Flight, National Aeronautics and Space Administration under Contract NASw-417.

TABLE OF CONTENTS

ABSTRACT

Photographic meteor data published by McCrosk y and Posen are analyzed using a method similar to one suggested by Orrok. It is found that, to a first approximation, the mass and velocity distribution functions are independent. Least squares analysis leads to a cumulative mass distribution of $\log N(m^{-2}sec^{-1}) = - \log m - 17.1$ where N is the cumulative flux of photographic meteors into the Earth's atmosphere having a mass of m kilograms or greater in good agreement with an earlier study of satellite and radar data by the writer. An independent check on the consistency of this distribution is carried out with favorable results. The velocity distribution is discussed using a very simple model for the distribution of orbital elements. It is then possible to define, for the first time, an analytic expression for the joint mass and velocity distribution function of photographic meteors. The result is applied to calculate various quantities of aerospace interest. The average meteor velocity is found to be 20 Km/sec, and analytical expressions for the penetration flux and the influx of meteor momentum are derived. The problem of the Earth's gravitational focusing is briefly considered and is found to be insignificant for these meteors.

SUMMARY

The meteoroid environment of the Apollo Program is subject to considerable uncertainties. This is due, on the one hand, to a scarcity of direct experimental measurements of the penetrating flux and, on the other hand, to uncertainties in estimates based on indirect information. The flux range of interest for Apollo consists of meteoroids which enter the Earth's atmosphere with a frequency of from 10^{-11} to 10^{-6} times per square meter per second. An important anchor point at the high end of this flux is provided by the Explorer and Pegasus direct measurements. The present study has been undertaken to provide a useful anchor point at the low end of this flux range, just beyond the significant range for Apollo.

Photographic meteor data published by McCrosk y and Posen comprise a statistically highly valuable sample of 2,529 meteors. A method of analysis, due to Orrok, is employed here and the sample is divided, accordingly, into meteor mass distributions at constant velocity and velocity distributions at constant mass. With this method it is shown that the meteor mass and velocity distributi ons are independent to a good first approximation, as Orrok has earlier suggested. An important advantage of the method is that a much larger fraction of the total sample becomes accessible for analysis than has been possible before without having to introduce weighting factors which, due to their largely intuitive character, comprise a major source of uncertainty in the existing "state-of-the-art."

Least square analysis leads to a cumulative mass distribution of $\log N\ (M^{-2}sec^{-1}) = -\log m - 17.1$ where N is the cumulative influx of photographic meteors into the Earth's

atmosphere having a mass of m kilograms or greater in good agreement with an earlier estimate by the writer using mainly satellite and radar data. An independent check on the consistency of this distribution with the raw data is carried out with favorable results.

The velocity distribution is discussed using a simple model for the distribution of orbital elements. Using some of the results obtained during the analysis of mass distributions it becomes possible to define for the first time a joint mass and velocity distribution (equation 4.3.6 in the text) of photographic meteors. The results are then applied to calculate several quantities of aerospace interest.

The penetrating flux, derived from the model, is of particular interest because it provides a fixed anchor point in the flux range of 10^{-12} m^{-2} sec^{-1} to 10^{-15} m^{-2} sec^{-1}. This is indicated in the summary chart, Figure S, following this discussion. It can be seen, from the figure, that the penetrating flux derived from the present model agrees to within a factor of about 3 with an earlier estimate by the writer based mainly on satellite data. It is, therefore, satisfying to note that when the uncertainties in the present penetrating flux are extrapolated in Figure 5, the Pegasus (5 or more orders of magnitude higher in flux) data are within the margins of error. The unrevised NASA model is seen to diverge considerably from the main trend of satellite penetration measurements as well as penetration flux estimates based on radar data and the present results. It can further be seen, in the figure, that the penetrating flux estimated from microphone measurements is high. Because of their highly uncertain nature, penetrating flux estimates based on the influx rates of relative visual magnitudes have not been plotted in the figure.

Other results of this paper are the determination of an average meteor velocity of 20 Km/sec with a root mean square deviation of 7 Km/sec and an analytical definition of the influx of meteor momentum. Lastly, the effect of the Earth's gravitational focusing is considered and is found to be small, resulting in a decrease in flux of the order of 30% at infinity.

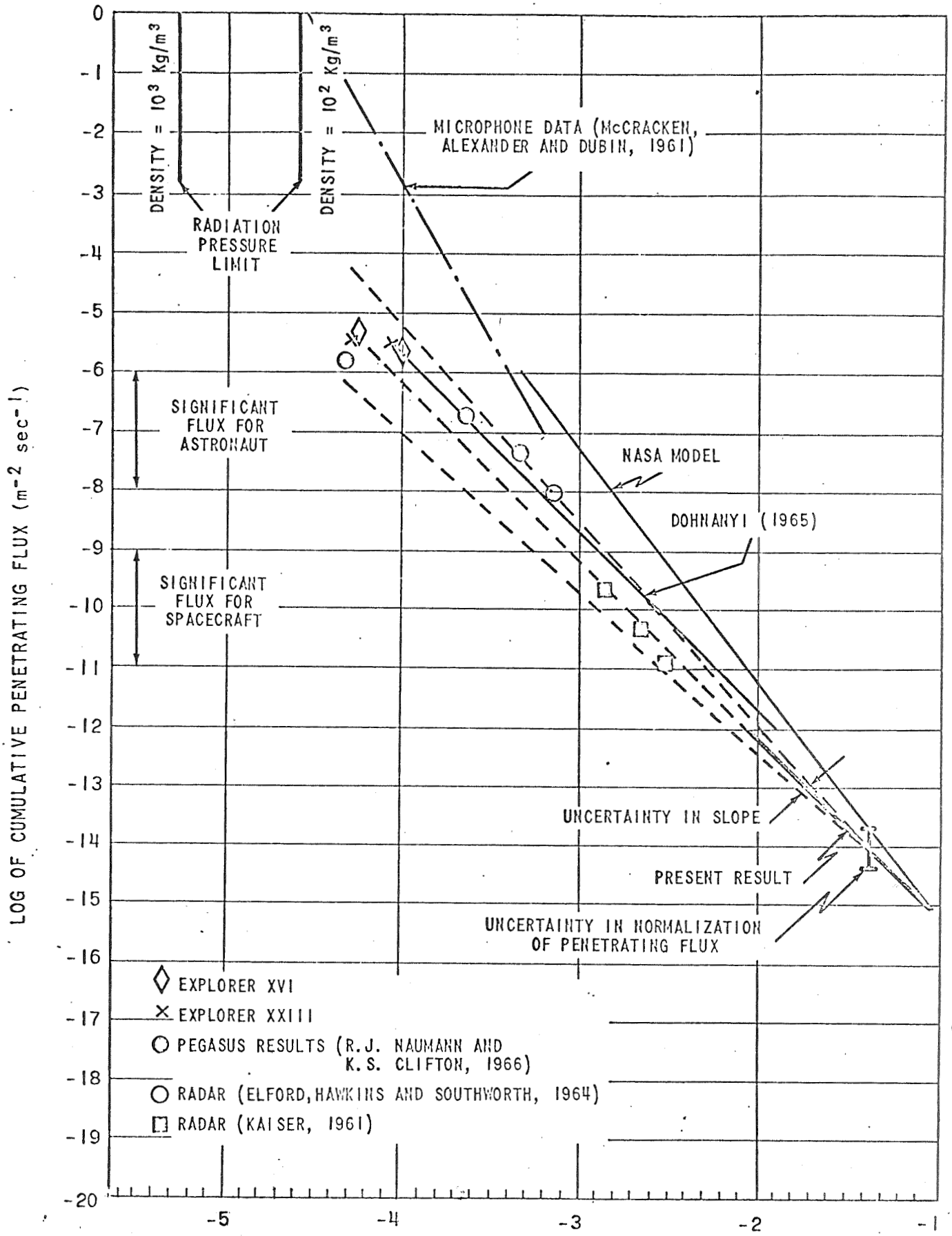
LOG OF CUMULATIVE PENETRATING FLUX (m^{-2} sec^{-1})
0
-1
-2
-3
-4
-5
-6
-7
-8
-9
-10
-11
-12
-13
-14
-15
-16
-17
-18
-19
-20
DENSITY = 10^3 Kg/m^3
DENSITY = 10^2 Kg/m^3
RADIATION PRESSURE LIMIT
MICROPHONE DATA (McCRACKEN, ALEXANDER AND DUBIN, 1961)
SIGNIFICANT FLUX FOR ASTRONAUT
SIGNIFICANT FLUX FOR SPACECRAFT
NASA MODEL
DOHNANYI (1965)
UNCERTAINTY IN SLOPE
PRESENT RESULT
UNCERTAINTY IN NORMALIZATION OF PENETRATING FLUX
EXPLORER XVI
EXPLORER XXIII
PEGASUS RESULTS (R.J. NAUMANN AND K.S. CLIFTON, 1966)
RADAR (ELFORD, HAWKINS AND SOUTHWORTH, 1964)
RADAR (KAISER, 1961)
-5
-4
-3
-2
-1
LOG OF PENETRATING THICKNESS IN METERS OF EQUIVALENT ALUMINUM

FIGURE - S

MODEL DISTRIBUTION OF PHOTOGRAPHIC METEORS

I. Introduction

The model meteoroid environment of the Apollo Program is subject to considerable uncertainties.* This is due mainly to a scarcity of direct observational information regarding the mass and velocity distribution of meteoroids. An improvement in the definition of the meteoroid mass distribution and a definition of a model velocity distribution would therefore lead to increased confidence in the Apollo Model Environment. Estimates of mass distribution of photographic meteors have been given in the past (see McKinley, 1961, for a review) and were originally based on indirect evidence (e.g., distribution of relative visual magnitudes). After Hawkins and Southworth (1958) reduced 360 meteors a direct analysis became possible. Using this sample Hawkins and Upton (1958) obtained the result that the cumulative influx of photographic meteors into the Earth's atmosphere is proportional to the - 1.34 power of the meteor mass. More recently Dalton (1965) has recalculated the masses of these meteors using Öpik's method and obtained a similar result. Joint mass and velocity distributions have not, however, been given in the literature.

McCrosk y and Posen (1961) have published the orbital elements of 2529 photographic meteors.** The sample comprises 2174 meteors reduced by the authors using the graphical method (McCrosk y, 1957) and 355 meteors reduced by Jacchia using a more accurate method (Whipple and Jacchia, 1957). In view of the high statistical value of the sample, it appeared worth while to undertake a systematic study of the McCrosk y and Posen meteors in order to define their mass and velocity distribution.

---

*See, e.g., Dohnanyi (1965) for a recent review and for references.

**The authors have kindly made available a set of their IBM data cards used in this study.

In an unpublished study, Orrok (1964) has constructed plots of mass distributions at constant geocentric velocity and geocentric velocity distributions at constant mass of the McCroskey and Posen meteors. Inspection of these plots led him to conclude that the mass distribution function at constant velocity is similar for the different velocity intervals he considered. Orrok further suggested (private communication) that a more detailed treatment may reveal that the mass and velocity distributions are independent.

The method used in this study is similar to the one employed by Orrok to investigate mass distributions at constant velocity and velocity distributions at constant mass. Details of the procedure are given in Section 2 of this paper. A careful study of the data indicates that, within a reasonable approximation, the mass and velocity distributions can indeed be considered independent.

The mass distribution of the McCrosk y and Posen meteors at different velocities is considered in detail in Section 3. Least squares analysis of mass distributions at 16 different velocity intervals indicates that the cumulative distribution is proportional to the - 1 power of the meteor mass. This is somewhat lower than the - 1.34 power obtained by Hawkins and Upton. The constant of proportionality is then determined from earlier work (Hawkins and Upton, 1958).

In Section 4 of this paper, we treat the velocity distribution of the meteor sample. The qualitative form of the distribution is discussed in terms of a simple theoretical model. Results from this section are then employed to derive a semi-empirical velocity distribution which is analytically defined with a least squares fit. Next a joint mass and velocity distribution is obtained for the first time which permits the analytical estimation of various derived quantities.

In Section 5 we consider the distribution of photographic magnitudes of the McCrosk y and Posen meteors. A simple mathematical treatment indicates a mass influx rate in complete qualitative agreement with the results of our least squares analysis.

Engineering applications of the results are discussed in Section 6. The average meteor velocity is found to be 20 Km/sec. The penetration flux is calculated and compared with other estimates. Finally, a brief discussion of the momentum influx and gravitational focusing are included.

2. Treatment of the Data

The 2529 meteors whose orbital elements were published by McCrosk y and Posen (1961) include the 355 meteors precisely reduced by Jacchia and 115 shower meteors that were partially reduced by the graphical method. Since this analysis will be concerned with sporadic meteors only, these 115 meteors as well as any additional shower meteors in the sample have been omitted. Meteors whose masses have not been determined are also excluded; the result is a sample of 2,039 sporadic meteors.

The masses of the McCrosk y and Posen meteors have been computed with the use of the formula*

$$m = \frac{2}{\tau_o V^3} \int_o^T I \, dt \qquad (2.1)$$

where m is the meteor mass, τ_o a constant, called the luminous efficiency, T is the lifetime of the meteor and I is the intensity of light emitted.

*The formula actually used is an approximation to Eq. 2.1 proposed by Hawkins (1957) for data reduction purposes.

The value of τ_o has recently been revised by Verniani (1964); the new value ($\tau_o = 10^{-19}$ c.g.s.) is $\frac{1}{6.46}$ of the old value with an estimated uncertainty of the order of 2. The masses of the McCrosky and Posen meteors given by Eq. 2.1 with the old value of τ_o have been multiplied here by 6.46 in order to make them coincide with the more recent mass scale. All masses quoted in this paper are in accordance with the new value of τ_o.

In what follows, a method of analysis suggested by Orrok (1964) is employed inasmuch as the data are separated into groups of different mass and velocity ranges. This then permits a study of mass distributions at constant velocity and velocity distributions at constant mass. The data have been divided into 20 logarithmically equal velocity intervals and 26 logarithmically equal mass intervals.

The gross features of the mass distribution as a function of velocity are summarized in Fig. 1 which is a plot of the meteor masses versus frequency on a doubly logarithmic plot. The outermost curve represents all the meteors; each successive plot is obtained by subtraction of successive velocity groups from the total, as indicated. It can be seen that each group of meteors has a similar distribution. The number of meteors in a given velocity group first increases (from right to left, in the figure) with decreasing mass, reaches a peak and then dimishes again becoming negligible for masses smaller than 10^{-6} Kg.

Treating the data in a different manner, Orrok (1964) has also observed these features; in what follows, our discussion concurs to a large extent with that of Orrok.

The increase in the number of meteors with decreasing mass (right hand side of the figure) is to be attributed to the natural distribution of meteors. It is generally assumed that meteor masses are distributed according to an exponential law, of the form

$$f_m(m)dm = Am^{-\alpha}dm \tag{2.2}$$

where $f_m(m)dm$ is the number of meteors having a mass between m and m + dm, A and α are constants and m is the meteor mass. Accordingly, the approximately linear rise in the mass distribution (from right to left on the figures) is due to a meteor mass distribution of the form Eq. 2.2 .

The "bending over" of these curves (going from right to left on the diagram) is the result of instrumental selection effects. The brightness of the meteor trail on the photographic plate is a function of the meteor mass and velocity as well as other parameters. As the brightness of the image becomes comparable to the stellar background on the photographic plate, an increasing number of faint meteors will escape detection. Eventually, for small enough meteors, the image is so faint that it is lost to the background altogether.

An interesting feature of the curves in Fig. 1 is that the mass value at which the distribution curve "bends over" (from right to left) decreases with increasing velocity. More specifically, in the mass range of 10^{-5} to 10^{-3} Kg, the curve representing all meteors is so heavily influenced by instrumental selection that no meaningful distribution can be defined. At higher velocities, however, an approximate power law mass distribution is evident in this same mass range. Furthermore, the masses of the smaller meteors (at higher velocities) appear to be distributed with the same slope (on log-log plot), but at masses in

excess of 10^{-3} Kg, a break in the slope may be present defining a "shallower" distribution for the heavier meteors.

The velocity distribution of the meteors is plotted in Fig. 2. Meteors with different mass ranges are plotted, in this figure, as a function of velocity. It can be seen, from the figure, that the heavier meteors have similar velocity distributions while the lighter meteors are clustered into the high velocity region. This tendency gives a totally different number vs. velocity distribution for the whole sample than is observed for the heavier meteors which have a sufficiently bright trail to be detected at low velocities.

The claim is now introduced, that, to a good first approximation, the differences in the shape of the number distribution as a function of mass or velocity (Fig. 1 and 2) for different groups is not a real effect but is due to instrumental selection, as has been pointed out earlier. This means that the curves in Fig. 1 are taken to represent the true distributions (without requiring corrections) for a given velocity group down to that value of the mass at which meteors are beginning to escape detection on the photographic plate. Similarly, on Fig. 2, we claim the curves to represent the true velocity distributions for a given mass group where for the smaller mass groups a minimum velocity exists at which the detection of the meteor trails is no longer assured. Using this model, we shall proceed in constructing a distribution function

$$f_{m,v}(m,v)\,dmdv = f_m(m)\, f_v(v)\, dmdv \tag{2.3}$$

where $f_{m,v}(m,v)$ is the number of meteors having a mass between m and m + dm and velocity between v and v + dv. $f_m(m)$ and $f_v(v)$

are independent distribution functions of the mass and velocity, respectively. We follow usual practice in assuming further that the mass distribution $f_m(m)$ is given by the simple power law, Eq. 2.2 .

3. Mass Distribution

In this section, we shall determine the values of the constants in the mass distribution $f_m(m)$. This will be accomplished by a least squares fit to the data. We use 16 of the 20 different velocity groups; four groups do not contain enough meteors to be statistically significant and they belong to velocities either less than the Earth escape velocity of 11.2 Km/sec or in excess of the solar excape velocity of 72 Km/sec. McCroskey and Posen attribute their presence to experimental errors in the reduction process.

Figure 3 through 18 are plots of the meteors under discussion. It can be seen that as the velocity increases, the distribution includes more light meteors and less heavy ones. This implies (cf., Fig. 2) that the true meteor distribution diminishes at higher velocities. The relative paucity of small mass meteors at low velocities can be attributed to difficulties of their detection.

The number of meteors in each mass range element is indicated by the histograms. Since these plots are logarithmic, the distribution function $f_m(m)$ does not coincide* with the histograms and its value at each interval is indicated by solid black circles. Each "step" of the histogram is the integral of

---

*This can be seen by recalling that $f_m(m)dm$ is the number of meteors having a mass between m and m + dm and that on our logarithmic plot the ratios of adjacent mass intervals are equal but not the mass intervals themselves.

$f_m(m)$ over the respective elemental mass range. Taking

$$(3.1) \qquad f_m(m) = Am^{-\alpha}$$

the number of meteors having a mass between m_1 and m_2 is

$$(3.2) \qquad N_{12} = \int_{m_1}^{m_2} f_m(m)dm = \frac{Am_1^{-\alpha+1}}{\alpha-1}\left(1 - \left[\frac{m_1}{m_2}\right]^{\alpha-1}\right)$$

$$= \text{constant} \times m_1^{-\alpha+1}$$

since m_1/m_2 is constant for a logarithmically equally divided mass scale. Eq. 3.2 then represents the histograms.

The straight line through the figures is a least squares fit to the data of Eq. 3.2 . The number referred to as "slope" is the quantity $1-\alpha$ and is given for each velocity interval.

By "range of fit" we indicate the mass range over which the data have been fitted, together with the number of meteors used. The dashed horizontal line indicates the extent of a second range over which a least squares program has been carried out where most of the infrequent heavy meteors have been rejected. This second least squares program is of an auxiliary nature and will be used only to estimate the uncertainty in our results.

The average value obtained for the slope, $\alpha-1$, is $.93 \pm .15$. The slopes for individual velocity classes are plotted against velocity in Fig. 19 together with their standard estimators of error. It can be seen, from this figure, that the slopes are distributed fairly randomly with the velocity.

The second least squares program, where most of the heavy and less numerous meteors have been excluded, yielded an average slope of $1.06 \pm .05$. We, therefore, round off upwards the value of $\alpha-1$ to give $\alpha-1 \tilde{=} 1$. Whence, the mass distribution becomes

$$f_m = m^{-2} \times \text{constant} \tag{3.3}$$

and the conventionally quoted cumulative mass distribution is

$$\log N = - \log m + B \tag{3.4}$$

with an uncertainty of about 10% in the slope.

To define the value of the normalization constant B, we shall follow Hawkins and Upton (1958). These authors estimated the mean rate of observing sporadic meteors at 2.65 per hour and a collection area of 5,980 Km^2 for the Super-Schmidt cameras. While these authors do not define the uncertainty in this estimate, the approximately sinusoidal diurnal variation (Hawkins and Upton, 1958) leads one to expect a root mean square deviation of the order of 30%.

The total number of meteors used here is 2,059. This number includes 132 meteors with a mass equal to or larger than 10^{-3} Kg (i.e., 1 gm). Hence the value of B is

$$B = - 17.10 \tag{3.5}$$

and the cumulative flux is,

$$\log N = - \log m - 17.10 \tag{3.6}$$

in MKS units.

We have plotted, in Fig. 20, the result of the least squares estimates Eq. 3.6, together with earlier estimates of the cumulative flux. The curve marked Whipple, represent Whipple's (1963) cumulative flux model

$$(3.7) \qquad \log N = -1.34 \log m - 18.5 + 2.68 \log \frac{.44}{\rho}$$

where ρ is the specific gravity of the meteor. Fig. 20 contains a plot of Eq. 3.7 with $\rho = .44$. The curve, labeled Dohnanyi (1965) is an extrapolation of Dohnanyi's estimate, based mainly on satellite and radar data and is given by

$$(3.8) \qquad \log N = -\log m - 16.9$$

It can be seen, from the figure, that our least squares fit agrees excellently with the extrapolation of Dohnanyi's 1965 estimate, the latter being slightly higher. In view of the uncertainties in Dohnanyi's estimate (Dohnanyi, 1965), however, this agreement is somewhat fortuitous. Good quantitative agreement exists between the least squares fit and Whipple's 1963 estimate for $\rho = .44$ and a mass range of about 10^{-5} to $10^{-3.5}$ Kg. The qualitative agreement is, however, poor because of the different coefficients for log m as given in Eq. 3.6 and 3.7 . The least squares fit is low compared with Whipple (1963) for $\rho = .44$ and mass smaller than about $10^{-4.5}$ Kg and is high for masses larger than about 10^{-4} Kg.

4. Velocity Distribution

4.1 Empirical Distribution

We shall, in this section, discuss two problems related with the velocity distribution. Using the results of the previous section, we shall first correct the velocity distribution for instrumental error and define the resulting model distribution analytically. Finally, in Section 4.2, the theoretical significance of the distribution is discussed.

In the previous section, the semi-empirical formula

$$f_m(m)dm \doteq \text{constant } m^{-2}\, dm \tag{4.1}$$

was obtained, where dN is the number of meteors having a mass between m and m + dm. Assuming that this is the true mass distribution for each of the velocity intervals used, one can write, for the j^{th} velocity interval

$$N_{12}{}^{j} = \int_{m_1}^{m_2} \text{constant } m^{-2}\, dm = c_j m_1^{-1} \left(1 - \left[\frac{m_1}{m_2}\right]\right) . \tag{4.2}$$

Here $N_{12}{}^{j}$ is the number of meteors used for the empirical fit having masses between m_1 and m_2 Kg in the j^{th} velocity interval. c_j is then the integral of the velocity distribution over the j^{th} velocity interval. Since N_{12}, m_1 and m_2 are known, we can obtain, empirically, the quantities c_j. The result is plotted in Figure 21 where the solid curve is a plot of the quantities c_j. It can be seen, from the figure, that starting with Earth escape velocity, the number of meteors (at constant mass) increases with the velocity. It reaches a peak value in the velocity interval of 16.4 to 18.4 Km/sec and then decreases until a velocity of about 46.1 Km/sec is reached. At this velocity, a change in the

distribution is indicated until the retrograde hyperbolic velocity at 72 Km/sec is reached (beyond which velocity no statistically significant number of meteors is found).

The differential velocity distribution can readily be obtained by noting that c_j can be written as

$$(4.3) \qquad c_j = \text{const} \int_{v_j}^{v_{j+1}} f(v)\, dv$$

where f(v) is the velocity distribution function. For a small enough velocity interval, the integral in Eq. 4.3 can be written, approximately, as

$$(4.4) \qquad \int_{v_j}^{v_{j+1}} f(v)\, dv \approx f(\bar{v}_j)\,(v_{j+1} - v_j) \equiv f(\bar{v}_j)\,\Delta v_j$$

where $\bar{v}_j$ is the average value of v over the interval. Whence, f(v) can be expressed as

$$(4.5) \qquad f(v_j) \approx \left|\frac{c_j}{\Delta v_j}\right| \quad \text{x constant} \quad .$$

The velocity distribution f(v) is plotted in Fig. 21 as a dashed curve. It exhibits the same qualitative features as the distribution of the quantities c_j, except that f(v) is steeper in the higher velocity region.

Fig. 22 is a plot of the quantities c_j so normalized as to present a direct basis for comparison with the McCroskey and Posen data. This has been accomplished with use of Eq. 4.2.

where N_{12} is calculated as a function of the quantities c_j for a given m_1/m_2. When $m_1 << m_2$, then Eq. 4.2 simplifies to

$$N_{12} \simeq c_j \, m_1^{-1} \tag{4.6}$$

Since the quantities c_j have been determined we can calculate the total number of meteors N_{12} in an arbitrary mass range m_1 to m_2 and velocity interval j which the McCroskey and Posen data should contain if all faint meteors would be detected.

We used three mass intervals, i.e., masses equal to or larger than 2.8×10^{-3} Kg, 6.1×10^{-4} Kg, and 10^{-4} Kg. The raw data (cf., Fig. 2) for these distributions is also plotted in Fig. 22 for comparison. Curves represent the McCroskey and Posen data and solid points represent the corrected distribution (Eq. 4.6) consistent with our model. The total number of McCroskey and Posen meteors have also been plotted for comparison. It can be seen that our model over-estimates the number of heavy meteors (mass $\gtrsim 10^{-3}$ Kg) but reproduces the distributions for smaller meteors rather well. The disagreement for heavy meteors is not serious in view of their small number and lower statistical significance. At low velocities, our curve is about two times higher than the actually observed number of meteors with masses equal to or larger than 10^{-4} Kg. This we attribute to the fact that many meteors in this range are not detected.

4.2 Theoretical Velocity Distribution

In this section, a discussion of the physical meaning of the velocity distribution is presented. More specifically, with the use of a very simple model, the gross features of the velocity distribution are reproduced.

The meteor velocity, V, near the Earth's surface can be expressed as

$$V = \sqrt{V_G^2 + 125} \tag{4.2.1}$$

where V_G is the geocentric velocity of the meteor in Km/sec, i.e., V_G is the velocity at which the meteor would be travelling near the Earth's surface if the Earth did not possess a gravitational field (which accelerates the meteor).

The quantity V_G can be expressed, in vector notation, as

$$\vec{V}_G = \vec{V}_H - \vec{V}_E \tag{4.2.2}$$

where $\vec{V}_H$ is the heliocentric velocity of the meteor (i.e., the meteor velocity relative the sun), $\vec{V}_E$ is the Earth's heliocentric velocity and has a mean (scalar) value of 29.8 Km/sec. It is readily seen that the scalar value of V_G is given by

$$V_G^2 = V_H^2 + V_E^2 - 2 V_E V_H \cos \phi \tag{4.2.3}$$

where ϕ is the angle between $\vec{V}_H$ and $\vec{V}_E$ (i.e., ϕ is the complement of the declination).

Two cases can at once be distinguished: when $\phi < 90°$, the meteor moves around the sun in the same sense as the Earth and its motion is known as direct; when $\phi > 90°$, the meteor moves around the sun in a sense opposite to the Earth's motion and its motion is called retrograde.

The quantities on the right hand side of Eq. 4.2.3 can now be expressed in terms of orbital parameters:*

$$V_H^2 = V_E^2 \left(2 - \frac{1-e}{p}\right) \tag{4.2.4}$$

$$V_H \cos \phi = \pm V_E \sqrt{p(1+e)}$$

where e is the eccentricity of the orbit and p is the perihelion distance (in astronomial units). These formulae are valid if the orbital inclination is zero (i.e., the meteor orbit is in the ecliptic). The + sign is to be used for direct orbits and the - sign for retrograde orbits. Restricting the inclination to 0° is not an untenably severe condition since most of the meteors have small inclinations (McCroskey and Posen, 1961).

Substitution of Eq. 4.2.4 into Eq. 4.2.3 gives, for direct orbits:

$$\frac{V_G^2}{V_E^2} = 3 - \frac{1-e}{p} - 2\sqrt{p(1+e)} \tag{4.2.5}$$

Consider the family of meteor orbits with p equal to 1.A.U.; Eq. 4.2.5 then becomes

$$\frac{V_G^2}{V_E^2} = 2 + e - 2\sqrt{1+e} \tag{4.2.6}$$

*For a derivation, see, e.g., Goldstein (1951).

These meteors may collide with the Earth at any angle $\phi \leq 90°$ and their orbit may intersect the Earth's orbit at as many as three points (depending on the eccentricity).

We notice, from Eq. 4.2.6 that $V_G = 0$ when e=0 indicating that in this case the meteor and Earth orbit coincide, as they should. We further notice that V_G^2 increases when e increases and reaches a maximum value

$$V_G = (\sqrt{2} - 1) V_E \tag{4.2.7}$$

when e=1. Since e > 1 represents meteors coming in from outside of the solar system and since no conclusive evidence has ever been presented regarding the existence of such meteors, we shall only consider orbits for which $e \leq 1$.

Knowledge of the distribution of eccentricities e now permits us to calculate the distribution of geocentric velocities due to this class of meteors.

Consideration of the data indicates, as has been pointed out by McCrosk y and Posen, that the eccentricities are distributed, approximately as

$$f_e(e) = \text{constant} \times e^2 \quad \text{for } e \leq 1 \tag{4.2.8}$$

where $f_e(e)$ is the distribution function of eccentricities, i.e., $f_e(e)de$ is the number of meteors having eccentricities between e and e + de.

Given $f_e(e)$, we now define* the distribution function $f_G(V_G)$ of V_G.

$$(4.2.9) \quad f_G(V_G) = \left(\frac{V_G}{V_E}\right)^2 \left(\frac{V_G}{V_E} + 1\right) \left(\frac{V_G}{V_E} + 2\right)^2 \quad \text{x constant}$$

valid for

$$(4.2.10) \quad 0 \leq \frac{V_G}{V_E} \leq \sqrt{2} - 1 \quad .$$

The corresponding distribution of the Earth entry velocity of the meteors is then

$$(4.2.11) \quad f_v(V) = V\sqrt{V^2-125}\left[\sqrt{V^2-125} + V_E\right]\left[\sqrt{V^2-125} + 2V_E\right]^2 \quad \text{x constant}$$

valid in the region

$$(4.2.12) \quad 11.2 \leq V \leq 16.6$$

where V is expressed in Km/sec.

It can be seen, from Eq. 4.2.11 that $f_v(V) = 0$ when $V = 11.2$ and then increases with V, reaching its largest value at the cutoff, i.e., at $V = 16.6$.

---

*See Appendix A for details.

We now consider the distribution of meteors having an Earth entry velocity higher than 16.6 Km/sec. The data indicate that the distribution of the heliocentric velocities is very strongly peaked near the solar escape velocity, indicating the presence of a large number of meteors with highly elongated orbits. We, therefore, turn our attention to meteors whose orbit has an eccentricity of approximately 1.

Letting e=1 in Eq. 4.2.5, we have:

$$\frac{V_G^2}{V_E^2} = 3 - 2\sqrt{2p} \qquad (4.2.13)$$

These meteors with parabolic orbits intersect the Earth orbit at two points when p<1 and at one point only (i.e., at perihelion) when p=1 and for p>1 do not intersect at all and whence they will not be considered here. Thus, the minimum geocentric velocity in Eq. 4.2.13 corresponds to the case when p=1.

$$V_G/V_E = \sqrt{3 - 2\sqrt{2}} \approx \sqrt{2} - 1 \qquad (4.2.14)$$

and the maximum value is obtained when p=0 ,

$$V_G/V_E = \sqrt{3} \qquad (4.2.15)$$

In the first limiting case (Eq. 4.2.14) we have meteors catching up with the Earth from behind, at perihelion. At the second limit (Eq. 4.2.15) we have meteors intersecting the Earth's orbit at 90°; the rest of the possibilities represented by Eq. 4.2.13 are intermediate between these limits.

The distribution of perihelia $f_p(p)$ of the McCrosk y and Posen meteors have a form

$$(4.2.16) \qquad f_p(p) = \text{constant } p^{1.5} \quad ,$$

approximately. Hence the V_G are approximately distributed as

$$(4.2.17) \qquad f_G(V_G) = V_G\left[3 - \left(\frac{V_G}{V_E}\right)^2 \right]^4 \quad \text{x constant} \quad .$$

The earth entry velocities, V, are then given by

$$(4.2.18) \qquad f_V(V) = V\left[3 - \frac{V^2 - 125}{V_E{}^2} \right]^4 \quad \text{x constant} \quad .$$

The range of velocities for which Eq. 4.2.18 is valid can be obtained from relations 4.2.14 and 4.2.15. The result is

$$16.6 < V < 52.8 \quad .$$

The velocity distribution function, Eq. 4.2.18 is a rapidly decreasing function of V. Over its region of definition, it has its largest value at V = 16.6 Km/sec and then decreases to zero at V = 52.8 Km/sec.

Figure 23 is a plot of the semi-empirical velocity distribution function obtained in the previous section together with $f_v(V)$ given by Eq. 4.2.11 and 4.2.18. The normalization constant for $f_v(v)$ has been chosen to represent, approximately, the number of meteors included in their respective intervals of definition. Since our sole purpose here is to discuss the qualitative features of the distribution, no attempt has been made to obtain a quantitative fit with the data.

It can be seen, from the figure, that in the velocity range of 11.2 Km/sec to 16.6 Km/sec the theoretical expression for $f_v(v)$ does indeed reproduce the gross trend of the data. The theoretical curve is concave downwards and the same trend is exhibited by the empirical curve. It, therefore, follows that the velocity distribution of meteors in the range of 11.2 Km/sec to 16.6 Km/sec can be explained by assuming that most meteors (in this velocity range) travel in direct orbits with small inclinations and perihelion distances of about 1A.U. They may collide with the Earth at perihelion in which case their radiant is directly opposite from the apex of the Earth's motion or they may "come in" at some other angle, less than 90°, if their orbit intersects the Earth's orbit away from perihelion.

The velocity distribution in the interval of 16.6 Km/sec to 52.8 Km/sec is due mainly to particles moving in very elongated (e is of the order of 1) and low inclination orbits. Both the theoretical and empirical curves are concave downwards, exhibiting similar trends. The theoretical curve underestimates the slow meteors relative to the faster ones, in this range. This is probably due to the simple approximation Eq. 4.2.16 of the distribution of perihelia. There is a fairly strong peak in the actual distribution* around p=1 which we have not included in the simple model and which would cause the value of $f_v(v)$ near the low velocity limit to be larger than given by Eq. 4.2.18 . Around 50 Km/sec the theoretical distribution becomes very small by comparison with the data. Also, at about this velocity, a marked change in the distribution of the data is indicated. This we attribute to the contribution of retrograde meteors, not included in the theoretical model. The retrograde meteors are seen to comprise a minor fraction of the total and their contribution becomes discernible at velocities in excess of 50 Km/sec. Their distribution appears to be markedly different from the direct meteors but a relative paucity of data in this region makes a detailed discussion of these meteors difficult.

*See McCrosk y and Posen (1961), Fig. 5.

4.3 Model Velocity Distribution

In this section we shall establish a simple analytical expression for the semi-empirical velocity distribution. Rather than refine the somewhat cumbersome formulas Eqs. 4.2.11 and 4.2.18 we shall fit the empirical velocity distribution to a simple exponential function of the form

$$f(V) = A\ V^{a} \qquad (4.3.1)$$

A least squares fit* gives

$$f_V(V) = C \times V^{1.6 \pm .7}, \qquad 11.2 \leq V \leq 16.6 \qquad (4.3.2)$$

$$= C \times 1.61 \times 10^{7} \times V^{-4.3 \pm .3}, \qquad 16.6 \leq V \leq 72.2$$

with V in Km/sec and where the constants have been so chosen that the distribution function is continuous. The quality of the fit can be seen in Fig. 24 to be quite good. We have plotted, in the figure, the semi-empirical velocity distribution together with the least squares fit.

The normalization constant can be obtained by noting that

$$f_{m,v}(m,V) = f_m(m)\ f_V(v) \times \text{constant} \qquad (4.3.3)$$

where $f_{m,v}(m,v)$ is the joint mass-velocity distribution function. The mass distribution is then given by (using numerical values from Eqs. 4.3 and 4.4)

---

*The least squares fit gives a maximum at 17 Km/sec but because of theoretical reasons we shall choose the normalization constants in such a manner that the maximum occurs at a meteor velocity of 16.6 Km/sec.

$$(4.3.4) \qquad f_m(m) = \int_{11.2}^{72.2} dV\, f_{m,v}(m,v) = 7.97 \times 10^{-18}\ m^{-2}$$

Integration of Eq. 4.3.2 then gives

$$(4.3.5) \qquad C = .971 \times 10^{-20}$$

The joint mass and velocity distribution then becomes,

$$(4.3.6) \qquad f_{m,v}(m,v) = .971 \times 10^{-20}\ m^{-2}\ V^{1.6}, \quad 11.2 \leq V \leq 16.6$$

$$= 1.56 \times 10^{-13}\ m^{-2}\ V^{-4.3}, \quad 16.6 \leq V \leq 72.2 .$$

5. Mass Distribution from Photographic Magnitudes

In this section the photographic* magnitude distribution of the McCrosky and Posen meteors is examined briefly to see what inferences, if any, can be drawn regarding the model mass distribution obtained in Section 3. More specifically, the exponent, α, of the mass distribution, will be calculated from the photographic magnitude distribution. Since this section utilizes a method which is independent from the one employed in Section 3, the results here serve as a check on the self-consistency of our model mass distribution.

It is generally accepted that the distribution of photographic magnitudes is of the form

*In what follows, by photographic magnitudes we mean absolute photographic magnitudes at maximum light.

(5.1) $$f_M(M)\, dM = \text{constant} \times r^M\, dM$$

where $f_M(M)\, dM$ is the number of meteors entering the Earth's atmosphere with photographic magnitudes between M and M + dM and r is a constant.

A theoretical relationship between the photographic magnitude M and meteor mass m can be expressed (Verniani, 1961; Jacchia et al 1965) in the form

(5.2) $$M = K_o + K_1 \log V + K_2 \log m + K_3 \log z_R \quad ,$$

where the various K's are constants, and z_R is the cosine of the zenith angle.

Introducing a mass, velocity and zenith angle distribution function of the form

(5.3) $$f_{m,v,z_R}(m,v,z_R)\, dm\, dV\, dz_R = m^{-\alpha} f_{v,z_R}(v,z_R)\, dm\, dV\, dz_R$$

one may proceed to express the exponent α in terms of the quantity r in Eq. 5.1 . To carry out this program, one has to, with the use of Eq. 5.2, eliminate the mass term in Eq. 5.3, paying due attention to the rules of transforming distribution functions (see the Appendix). When the resulting expression is integrated over all V and z_R, the result is the distribution function of photographic magnitudes.

One, therefore, has,

(5.4) $$f_{M,v,z_R}(M,v,z_R) = \frac{1}{|J|} f_{m,v,z_R}(m(M),v,z_R)$$

where J is the Jacobian of the transformation

$$J = \frac{\partial(M,v,z_R)}{\partial(m,v,z_R)} \tag{5.5}$$

Some algebra then gives

$$f_{M,V,z_R}(M,v,z_R) = 10^{-M(\alpha-1)/K_2} \times (\text{terms in V and } z_R) \tag{5.6}$$

Integrating this expression over all values of V and z_R gives, symbolically,

$$f_M(M) = \int dV \int dz_R \, f_{M,v,z_R}(M,v,z_R) = \text{constant} \times 10^{-M(\alpha-1)/K_2} \tag{5.7}$$

where $f_M(M)$ is the sought expression.

Comparing Eq. 5.7 with 5.1 then implies

$$10^{-\frac{\alpha-1}{K_2}} = r \tag{5.8}$$

or

$$-\frac{\alpha-1}{K_2} = \log r. \tag{5.9}$$

A semilogarithmic plot of the empirical photographic magnitude distribution of all 2,529 meteors published by McCrosk y and Posen is given in Fig. 25. The dashed straight line is a least squares fit to the "straight line" portion of the distribution. Our result is

$$f_M(M)\, dM = \text{constant}\ 10^{(.49 \pm .05)M}\, dM \tag{5.10}$$

Comparison of (5.10) with (5.7) gives

$$(5.11) \qquad .49 \pm .05 = -\frac{\alpha-1}{K_2} \quad .$$

The value of K_2 has been empirically determined by Jacchia et al as $K_2 = -2.25$. Hence, the value of the exponent for the mass distribution is

$$(5.12) \qquad \alpha = 2.1 \pm .1$$

which is somewhat lower than the widely used value of 2.34 given by Hawkins and Upton (1958).

This derivation of Eq. 5.12 is correct if the photographic magnitude scale of Jacchia et al coincides with that of McCrosk y and Posen. If a systematic difference exists between the two scales, than the value of - 2.25 for K_2 in Eq. 5.11 cannot be used without correcting the number on the left hand side of the equation for the discrepancy.

Kresak (1964) has pointed out a systematic difference between the photographic magnitude scales of McCrosk y and Posen and that appearing in 300 short trail meteors reduced by Hawkins and Southworth. Kresak found that this discrepancy is given by

$$(5.13) \qquad M \text{ (McCrosk } y) = .8 \text{ M (Hawkins)} - .18$$

No such comparison is available regarding the scale of Jacchia et al. Since, however, the graphic reduction method of McCrosky and Posen is less accurate than either of the other two, it may be assumed that Jacchia's scale of M coincides with that of the short trail method.

$f_M(M)$ can now be expressed in terms of the scale of magnitudes of the short trail method; combining Eq. 5.10 and 5.13 gives:

$$f_M(M) = \text{constant } 10^{(.39 \pm .04)\, M(\text{Hawkins})} \tag{5.14}$$

and

$$-\frac{\alpha-1}{K_2} = .39 \pm .04 \quad . \tag{5.15}$$

Substituting for K_2 now gives

$$\alpha = 1.88 \pm .09 \tag{5.16}$$

which is even lower than the value of 2.1 from Eq. 5.12. This value of α contains an error inasmuch our least squares fit Eq. 5.10 is based on 2529 meteors and 14% of these meteors have been reduced by Jacchia. Consistent with the postulate that Jacchia's scale is the same as Hawkins', $\alpha = 1.88$ is a lower limit.

This lower value of α is also in good agreement with the result, $\alpha = 2$, obtained in Section 3 of this study.

6. Aerospace Applications

In this section, we shall discuss several quantities of engineering interest that can be derived from Eq. 4.3.6. Of particular interest are the penetration flux, momentum flux and average velocity defined by our model.

6.1 Average Velocity

The average meteor velocity can be computed from Eq. 4.3.6 . One can write, by definition,

$$(6.1.1) \qquad \langle V \rangle = \left[\frac{\int dV \, f_{m,v}(m,v) \, V}{\int dV \, f_{m,v}(m,v)} \right]$$

where $\langle V \rangle$ is the expectation value of the velocity and the integral is to be taken over all velocities.

Using numerical values given in Eq. 4.3.6, the integral defining $\langle V \rangle$ can be evaluated to give,

$$(6.1.2) \qquad \langle V \rangle = 19.2 \text{ Km/sec} .$$

It is of interest to compute the root mean square velocity, i.e., the square root of the average velocity square. Again, by definition, we have

$$(6.1.3) \qquad \langle V^2 \rangle = \left[\frac{\int dV \, f_{m,v}(m,v) \, V^2}{\int dV \, f_{m,v}(m,v)} \right]$$

With the use of Eq. 4.3.6, the above relation can be evaluated, numerically; the result is

$$\sqrt{\langle V^2 \rangle} = 20.6 \text{ Km/sec} \quad . \tag{6.1.4}$$

The root mean square deviation of the velocity ΔV_{RMS} can be found from Eq. 6.1.4 and 6.1.2. One has:

$$\Delta V_{RMS} = \sqrt{|\langle V^2 \rangle - \langle V \rangle^2|} = 7 \text{ Km/sec} \tag{6.1.5}$$

and therefore, we can write, for our model

$$\text{average velocity} = 20 \pm 7 \text{ Km/sec} \quad . \tag{6.1.6}$$

The value of 20 Km/sec for the average velocity is considerably lower than the 30 Km/sec used for the Apollo model meteoroid environment. It is therefore recommended that the model should be revised accordingly.

6.2 Penetration Flux

It is of considerable interest to estimate the flux of particles penetrating a given thickness, T, of equivalent aluminum. Kinetic energy scaling will be employed here, i.e., the penetration depth is taken to be proportional to the two-third power of the particle kinetic energy. Computation of the influx of particle kinetic energy is therefore needed, to begin with.

For a given mass and velocity distribution $f_{m,v}(m,v)$ the joint velocity and kinetic energy ($\frac{1}{2}$ mv^2) distribution is

$$(6.2.1) \qquad f_{y,v} = \frac{f_{m,v}[m(y,v),v]}{|J|}$$

where y is the kinetic energy, i.e., $y = \frac{1}{2}$ mv^2 and where J is the Jacobian of the transformation for a function of m,v to be transformed into a function of y and v.

We shall be interested in the cumulative distribution function of the kinetic energy, i.e., we want to compute the quantity

$$(6.2.2) \qquad F_{>}(y) = \int_{y}^{\infty} dy \int dv \; f_{y,v}(y,v)$$

where $F_{>}(y)$ is the number of incident particles per square meters per second having a kinetic energy of y joules or greater.

Using Eqs. 6.2.1, 6.2.2, 4.3.6, one obtains

$$(6.2.3) \qquad F_{>}(y) = 1.73 \times 10^{-9} \times (\tfrac{1}{2} mv^2)^{-1}$$

where m is in Kg and v is in m/sec.

Dalton (1965) has recently obtained, empirically, the influx of kinetic energy of the meteors reduced by Hawkins and Southworth (1961) with the short trail method. After applying corrections for several selection effects, Dalton obtains a value of - .92 for the exponent of the kinetic energy in the

distribution function. Since the exponent in our expression (6.2.3) is -1, our model predicts a trend for the distribution within 8% of Dalton's results; the qualitative agreement is therefore excellent.

In order to compute the penetration flux, use is made of the Ames (Summers, 1959) penetration criterion in the form

$$T = 6.41 \left(\frac{\rho_P}{\rho_T}\right)^{1/3} \left[\frac{\frac{1}{2} mv^2 \cos^2 \theta}{\rho_T C_T^2}\right]^{1/3} \tag{6.2.4}$$

where T is the thickness of sheet metal penetrated by a projectile with density ρ_P and kinetic energy $\frac{1}{2} mv^2$ (in joules). The quantity ρ_T is the target density, C_T is the velocity of sound in the target and θ is the angle of incidence of the projectile (measured, as usual, from the normal to the target surface). In Eq. 6.2.4 we assumed that T equals 1.8 (Orrok, 1964) times the penetration depth into a semi-infinite target.

Choosing soft aluminum for a standard target, one has $\rho_t = 2.7 \times 10^3$ Kg/m^3 and $C_T = 5.1 \times 10^3$ m/sec. For the meteor density ρ_P we choose a value of 10^3 Kg/m^3 (Verniani and Hawkins, 1965), and we use a value of 1/2 for cos θ averaged over a hemisphere. Substitution of these quantities into Eq. 6.2.4 then gives,

$$T = 7.03 \times 10^{-4} \left[\frac{1}{2} mv^2\right]^{1/3} \tag{6.2.5}$$

Combining Eq. 6.2.3 with 6.2.5 then gives

$$(6.2.6) \qquad F_{>}(T) = 6.02 \times 10^{-19}\ T^{-3}$$

where $F_{>}(T)$ is the cumulative flux (in meters^{-2} sec^{-1}) of particles penetrating an aluminum sheet T meters or more in thickness. The uncertainty in the coefficient of Eq. 6.2.6 is of the order of $\times\ 10^{\pm.4}$ (Dohnanyi, 1965). The uncertainty in the exponent of T is due to the uncertainty in the exponent of m in the mass distribution and is of the order of 10%.

Using mainly satellite information, Dohnanyi (1965) has estimated the penetration flux and obtained

$$(6.2.7) \qquad F_{>}(T) = 2 \times 10^{-18}\ T^{-3}$$

with an uncertainty of the order of $10^{\pm.4}$ in the coefficient. It can be seen that Eqs. 6.2.7 and 6.2.6 are in very good agreement with each other; Dohnanyi's estimate is higher by about a factor of 3.

In an earlier paper, Orrok (1963) studied the relationship between the visual magnitude of meteors and their penetrating power; he obtained

$$(6.2.8) \qquad F_{>}(T) = 2 \times 10^{-17\pm1.2}\ T^{-3}$$

This relation is higher than Eq. 6.2.6 by a factor of about 30, the discrepancy being due to different normalization constants used by Orrok. According to the scale he used, the zero visual magnitude meteor traveling at 30 Km/sec has a mass of about 2.5×10^{-3} Kg while according to the more recent scale (Verniani, 1964) used here, such a meteor has a mass of about $.8 \times 10^{-3}$ Kg. Orrok has, furthermore, normalized his cumulative influx rate at the fifth visual magnitude using Whipple's (1958) estimate which is high compared with the McCrosk y and Posen Meteors.

6.3 Influx of Momentum

For certain applications, one needs to know the expression for the influx of particle momentum. Using our distribution function Eq. 4.3.6, one obtains

$$F_{>}(mv) = 1.625 \times 10^{-19}(mv)^{-1} \tag{6.3.1}$$

where $F_{>}(mv)$ is the cumulative influx per square meter per second of particles with momentum of mv units or larger. m is expressed here in Kg and v in Km/sec. The uncertainty in the exponent of mv is about 10%.

Dalton (1965) obtained an expression for the cumulative momentum influx with an exponent of - 1.09. This is seen to be within the margin of uncertainty of our present estimate and hence our exponent is in good agreement with that of Dalton.

6.4 Gravitational Focusing

For certain aerospace applications it is of interest to estimate the extent of particle concentration near Earth as a result of the Earth's gravitational attraction. Öpik (1951) has shown that

$$(6.4.1) \qquad \phi = \frac{\text{flux (at } R_1)}{\text{flux (at } R_2)} = \frac{V_a^2 + S_1^2}{V_a^2 + S_2^2}$$

where ϕ is the ratio of the flux at distance R_1 from the center of the Earth to the flux at a distance R (from the center of the Earth). V_a is the meteoroid geocentric velocity. The quantity S is given by

$$(6.4.2) \qquad S^2 = \frac{2G\mu}{R}$$

where G is the universal gravitational constant, μ the mass of the Earth and R is as defined above.

Taking R_1 at the surface of the Earth and expressing V_G in terms of the Earth entry velocity V one obtains, after some algebra,

$$(6.4.3) \qquad f_{m,v}(\varepsilon) = f_{m,v}(\text{at surface}) \times \left[1 + \left(\frac{1}{\varepsilon} - 1\right) \frac{125}{V^2}\right]$$

where $f_{m,v}(\varepsilon)$ is the mass and velocity distribution at a distance ε from the center of the Earth with ε expressed in units of Earth radii.

Using the model distribution Eq. 4.3.1 one can integrate Eq. 6.4.3 over all the velocities to obtain the mass distribution. The result is

$$(6.4.4) \qquad f_m(\varepsilon) = \left\{ 7.97 - (1 - \frac{1}{\varepsilon})\ 2.15 \right\} \times 10^{-18}\ m^{-2} \quad .$$

It can be seen that even at large distances from the earth ($\varepsilon = \infty$) the flux is decreased by less than 30% due to gravitational focusing. Since a difference of 30% is well within the margin of error, it is recommended that no distinction be made between near Earth and deep space fluxes of visual meteors as far as gravitational focusing is concerned.

7. Conclusion

The mass and velocity distribution of the McCrosk y and Posen meteors have been studied. Least square analysis leads to a distribution function given by Eq. 4.3.1 .

$$(7.1) \qquad f_{m,v}(m,v) = .971 \times 10^{-20}\ m^{-2}\ v^{1.6}, \quad 11.2 \leq v \leq 16.6$$

$$= 1.56 \times 10^{-13}\ m^{-2}\ v^{-4.3}, \quad 16.6 \leq v \leq 72.2$$

where m is the meteor mass in Kg and V is the meteor Earth entry velocity in Km/sec. The cumulative mass distribution then becomes

$$(7.2) \qquad F_{>}(m) = 7.97 \times 10^{-18}\ m^{-1}$$

where $F_{>}(m)$ is the cumulative influx of meteors per square meter per second having a mass of m Kg or more. This relation disagrees with Whipple's 1963 model, which has a mass exponent of - 1.34

and has been adopted into the NASA model. In the flux range of interest for Apollo, which includes flux values of $10^{-11} m^{-2} sec^{-1}$ or higher, Whipple's 1963 model (with $\rho = .44$) is high compared with an extrapolation of Eq. 7.2. The average meteor velocity, defined by Eq. 7.1 is 20 Km/sec. The Earth's gravitational focusing effect has been examined and no evidence for a strong near Earth concentration has been found for meteors in the photographic range.

1011-JSD-gdn

J. S. Dohnanyi

ACKNOWLEDGEMENTS

The writer is particularly indebted to J. M. Manville for performing all the programming and machine computation in this paper. Thanks are due to G. T. Orrok and N. W. Hinners for helpful suggestions; it is a pleasure to acknowledge helpful discussions with K. Baker and D. J. Kessler. R. J. Naumann has kindly communicated the latest Pegasus data, appearing in Fig. S, before publication.

REFERENCES

Dalton, C. C. NASA TMX-53325, 1965.

Dohnanyi, J. S., Bellcomm, TR-65-211-5, August 30, 1965.

Goldstein, H., "Classical Mechanics", Addison-Wesley Press, Inc., Cambridge, Mass., 1951.

Hawkins, G. S., Smithsonian Contr. Astrophys. 1, 207 (1957).

Hawkins, G. S. and R. B. Southworth, Smithsonian Contr. Astrophys. 2, 349 (1958).

Hawkins, G. S. and K. L. Upton, Astrophy. J: 128, 727 (1958).

Jacchia, L. G., F. Verniani and R. E. Briggs, Smithsonian Obs. Spec. Rep. No. 175, April 23, 1965.

Kresak, L., B.A.C., 15, 190 (1965).

McCracken, C. W., W. M. Alexander and M. Dubin, NASA TN D-1174 (December 1961).

McCrosk y, R. E., Smithsonian Contr. Astrophys, 1, 215 (1957).

McCros ky, R. E. and A. Posen, Smithsonian Contr. Astrophys. 4, 15 (1961).

McKinley, D. W. R., "Meteor Science and Engineering", McGraw-Hill, New York, 1961.

Naumann, R. J. and K. S. Clifton, NASA-TM, in preparation (1966).

Papoulis, A. "Probability, Random Variables, and Stochastic Processes", McGraw-Hill, Inc., New York, 1965.

Öpik, E. J., Proc. Royal Irish Acad. 54, 165 (1951).

Öpik, E. J., "Physics of Meteor Flight in the Atmosphere", Interscience Publishers, Inc., New York, 1958.

Orrok, G. T., Bellcomm TR, January 31, 1963.

Orrok, G. T., Bellcomm TR, January 31, 1964.

Summers, J. L., NASA TN D-94.

Verniani, F., Smithsonian Astrophys. Obs. Spec. Rep. No. 145, 1965; Smithsonian Contr. Astrophys., Vol. 8 No. 5, 1964.

Verniani, F. and G. S. Hawkins, Harvard Radio Meteor Project Research Report No. 12, 1965.

Whipple, F. L. and L. G. Jacchia, Smithsonian Contr. Astrophys. 1, 183 (1957)

Whipple, F. L.: "Vistas in Astronautics," pp. 115-124 (ed. Morton Alperin, Marvin Stern) Pergamon Press, N.Y., 1958.

Whipple, F. L., J. Geophysics. Res. 68, 4929 (1963).

APPENDIX

A-1. Transformation of Distribution Functions of One Variable

Suppose we have a distribution function of a variable x is given by $f_x(x)$ and wish to find the distribution function of the variable y given by

$$y = g(x). \tag{A-1-1}$$

If x can be solved for y, in the form

$$x_i = g_i^{-1}(y) \tag{A-1-2}$$

where $g_i^{-1}(y)$ denotes, symbolically, the i^{th} real root of x in Eq. A-1-1, then the distribution function of y, $f_y(y)$ is given by (for proof, see, e.g., Papoulis, 1965)

$$f_y(y) = \frac{f_x(x_1)}{|g'(x_1)|} + \ldots + \frac{f_x(x_i)}{|g'(x_i)|} + \ldots \frac{f(x_n)}{|g'(x_n)|} \tag{A-1-3}$$

where $x_1 \ldots x_i \ldots x_n$ are the n real roots of Eq. A-1 and where $g'(x) = dg(x)/dx$.

A-2. Transformation of Distribution Functions of Two Variables

Suppose we have a distribution function of two variables, x_1 and x_2, denoted by $f_{x_1x_2}(x_1,x_2)$. We wish to find the distribution function $f_{y_1y_2}(y_1,y_2)$ of the variables y_1 and y_2 given by

(A-2-1)
$$y_1 = y_1(x_1, x_2)$$
$$y_2 = y_2(x_1, x_2).$$

Suppose we can solve Eq. A-2-1 explicitly for x_1 and x_2 obtaining n real roots, say

$$x_1^1\ x_2^1,\ x_1^2\ x_2^2 \ \ldots\ x_1^n\ x_2^n$$

in terms of y_1 and y_2. Then the sought distribution function, $f_{y_1y_2}(y_2\ y_2)$ is given by (see Papoulis, 1965)

(A-2-2)
$$f_{y_1y_2}(y_1y_2) = \frac{f_{x_1x_2}(x_1^1\ x_2^2)}{|J(x_1^1\ x_2^1)|} + \ldots + \frac{f_{x_1x_2}(x_1^n\ x_2^n)}{|J(x_1^n\ x_2^n)|}$$

where $x_1^1\ x_2^1 \ \ldots\ x_1^n\ x_2^n$ are the n real roots of Eq. A-2-1 and where $J(x_1\ x_2)$ is the Jacobian of the transformation $\frac{\partial(y_1y_2)}{\partial(x_1x_2)}$ and is given, explictly, by the determinant

$$J(x_1x_2) = \begin{vmatrix} \frac{\partial y_1}{\partial x_1} & \frac{\partial y_1}{\partial x_2} \\ \frac{\partial y_2}{\partial x_1} & \frac{\partial y_2}{\partial x_2} \end{vmatrix}$$

Simple substitution of variables into these relations permits one to perform all the transformations of distribution functions used in this paper.

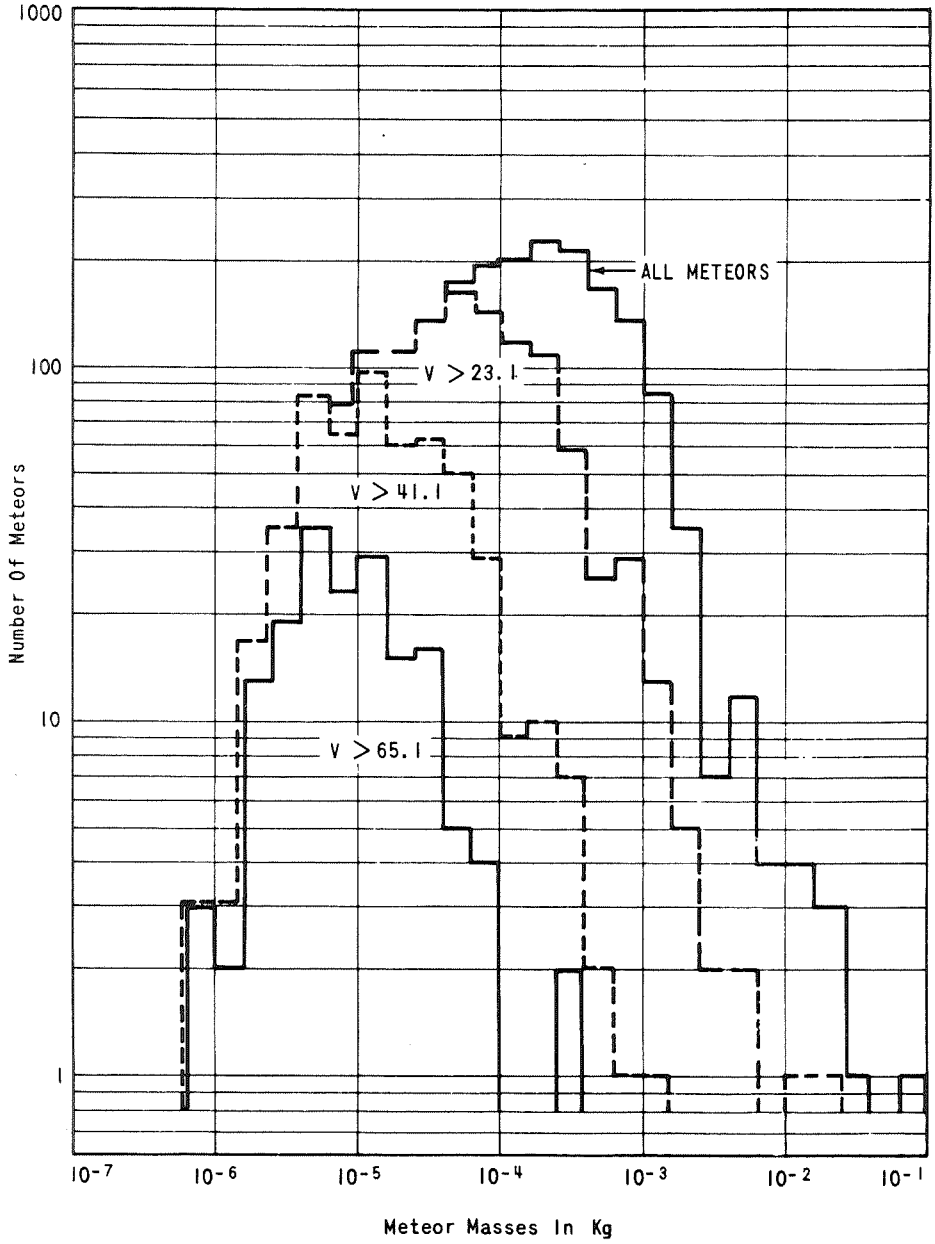

FIGURE 1 - DISTRIBUTION OF METEOR MASSES

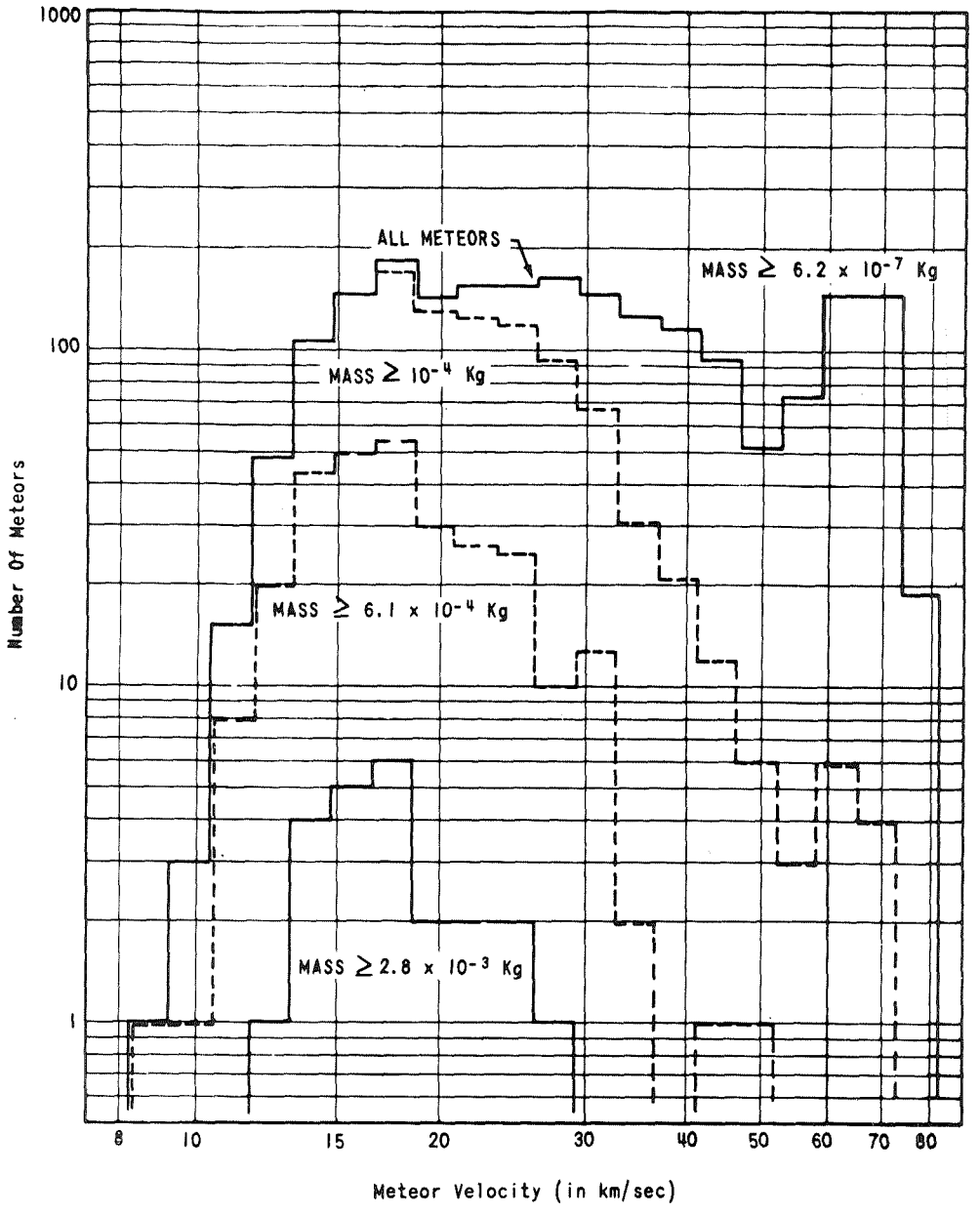

FIGURE 2 - DISTRIBUTION OF METEOR VELOCITIES

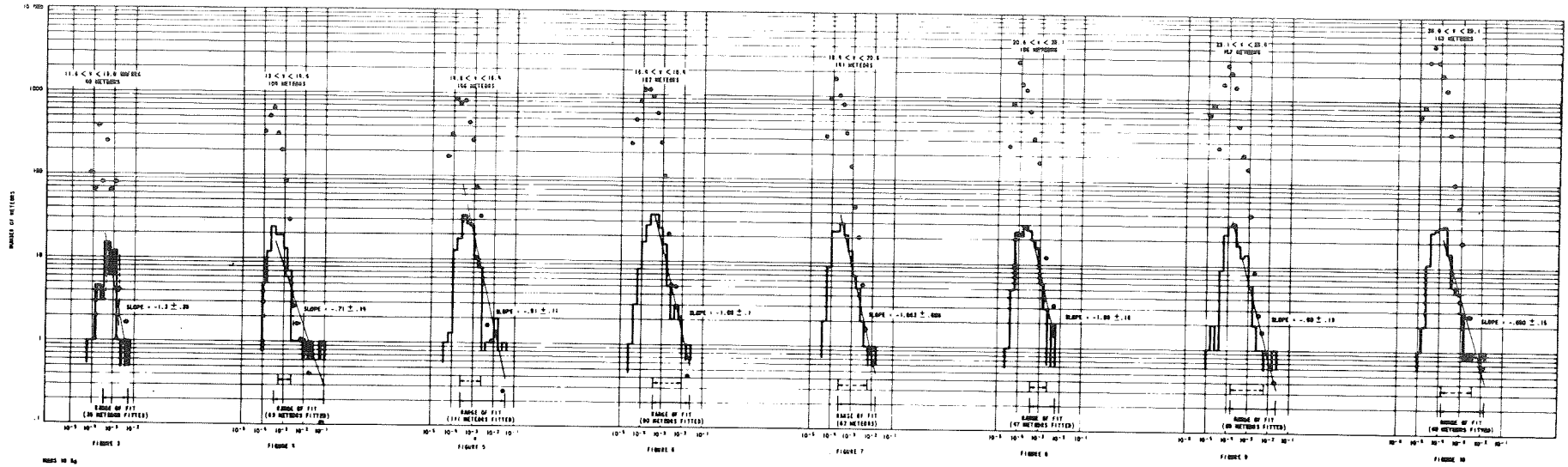

FIGURE 3 FIGURE 4 FIGURE 5 FIGURE 6 FIGURE 7 FIGURE 8 FIGURE 9 FIGURE 10

HISTOGRAMS REPRESENT THE NUMBER OF METEORS AS AN ELLIOT-HUGHES ROLLS RANGE; STRAIGHT LINES ARE LEAST SQUARES FITS TO THE HISTOGRAMS OVER A RANGE INDICATED. SOLID CIRCLES ARE THE MASS DISTRIBUTION FUNCTION AND DASHED HORIZONTAL LINES ARE THE RANGES OVER WHICH A LEAST SQUARES FIT (NOT SHOWN) FOR DISTRIBUTION FUNCTION HAS BEEN CARRIED OUT.

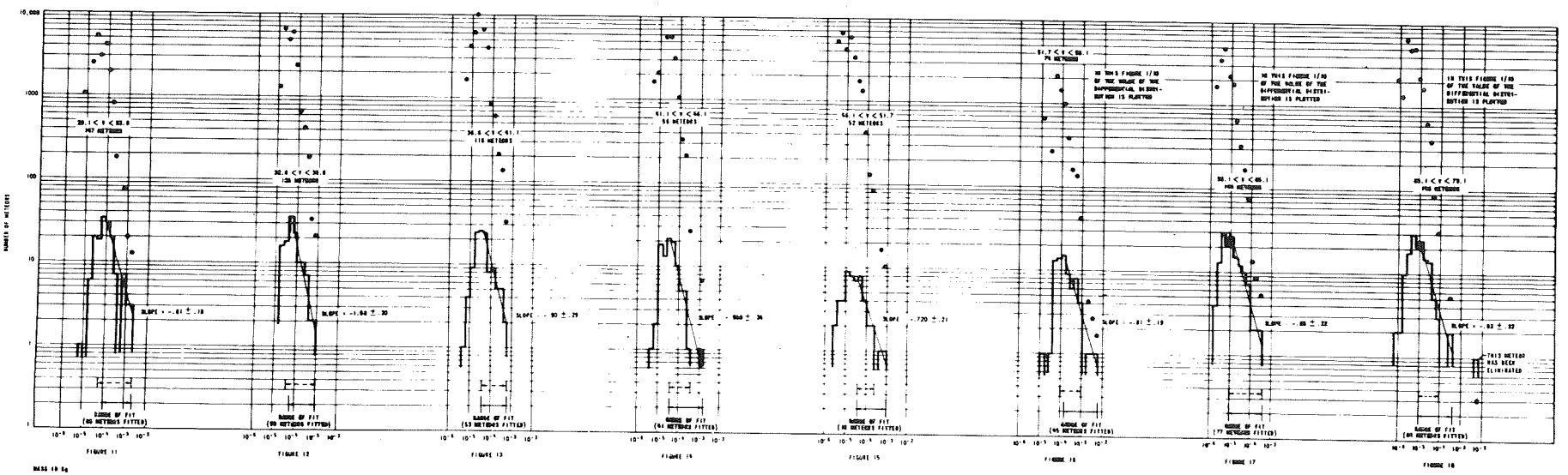

FIGURE 11 FIGURE 12 FIGURE 13 FIGURE 14 FIGURE 15 FIGURE 16 FIGURE 17 FIGURE 18

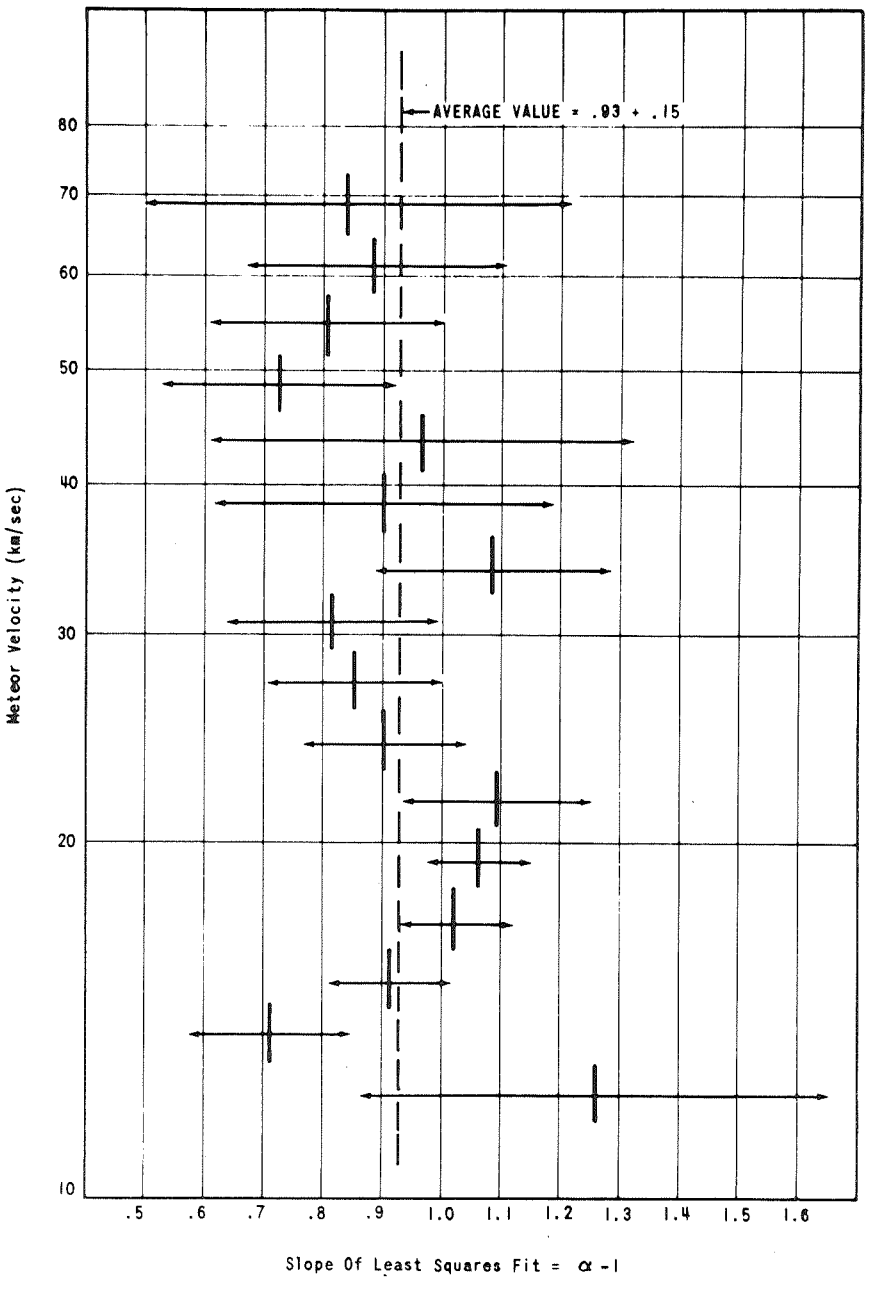
AVERAGE VALUE = .93 ± .15
Meteor Velocity (km/sec)
80
70
60
50
40
30
20
10
.5
.6
.7
.8
.9
1.0
1.1
1.2
1.3
1.4
1.5
1.6
Slope Of Least Squares Fit = α -1

FIGURE 19

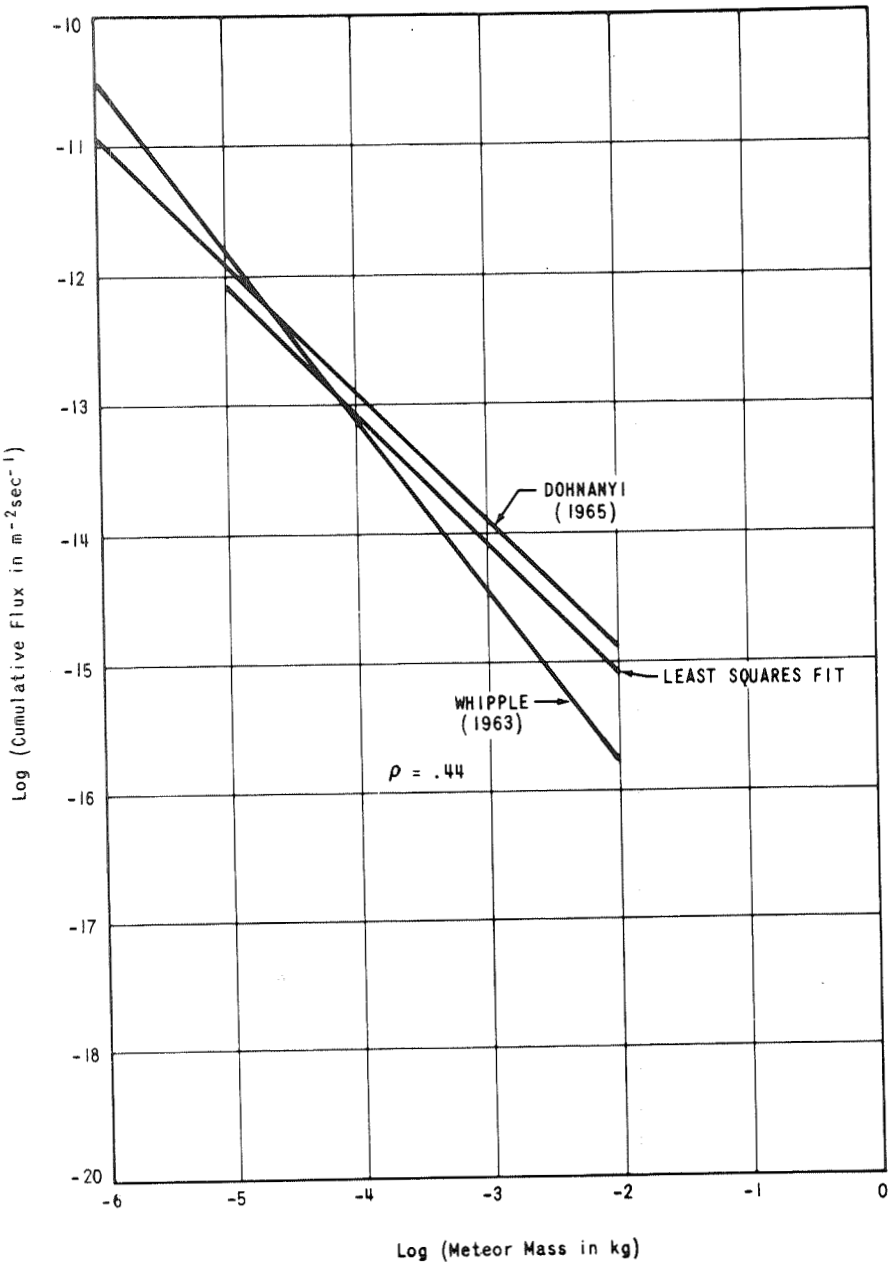
-10
-11
-12
-13
-14
-15
-16
-17
-18
-20
-6
-5
-4
-3
-2
-1
0
Log (Cumulative Flux in m^{-2}sec^{-1})
Log (Meteor Mass in kg)
DOHNANYI
(1965)
LEAST SQUARES FIT
WHIPPLE
(1963)
ρ = .44

FIGURE 20

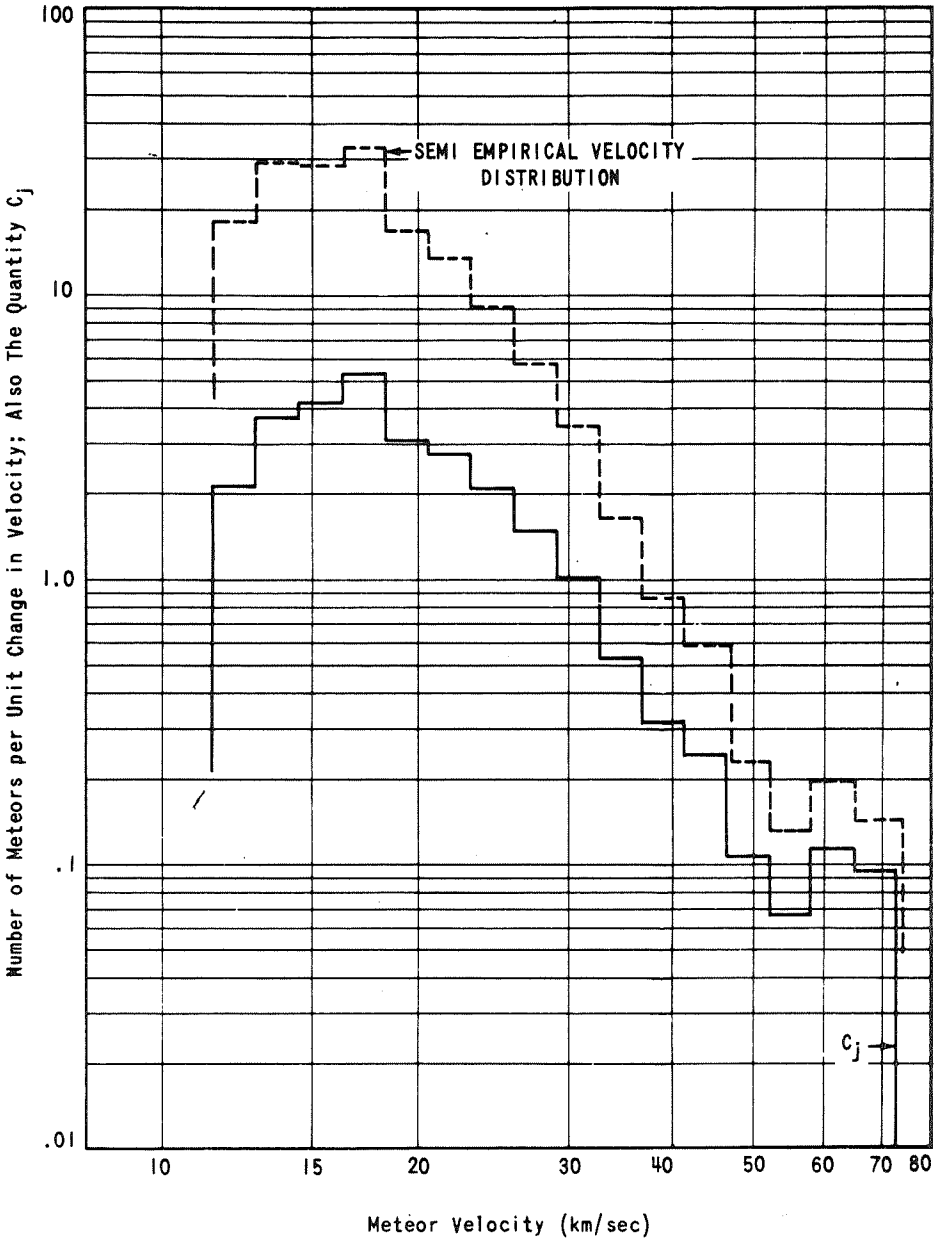
100
10
1.0
.1
.01
SEMI EMPIRICAL VELOCITY DISTRIBUTION
C_j
10
15
20
30
40
50
60
70
80
Number of Meteors per Unit Change in Velocity; Also The Quantity C_j
Meteor Velocity (km/sec)

FIGURE 21

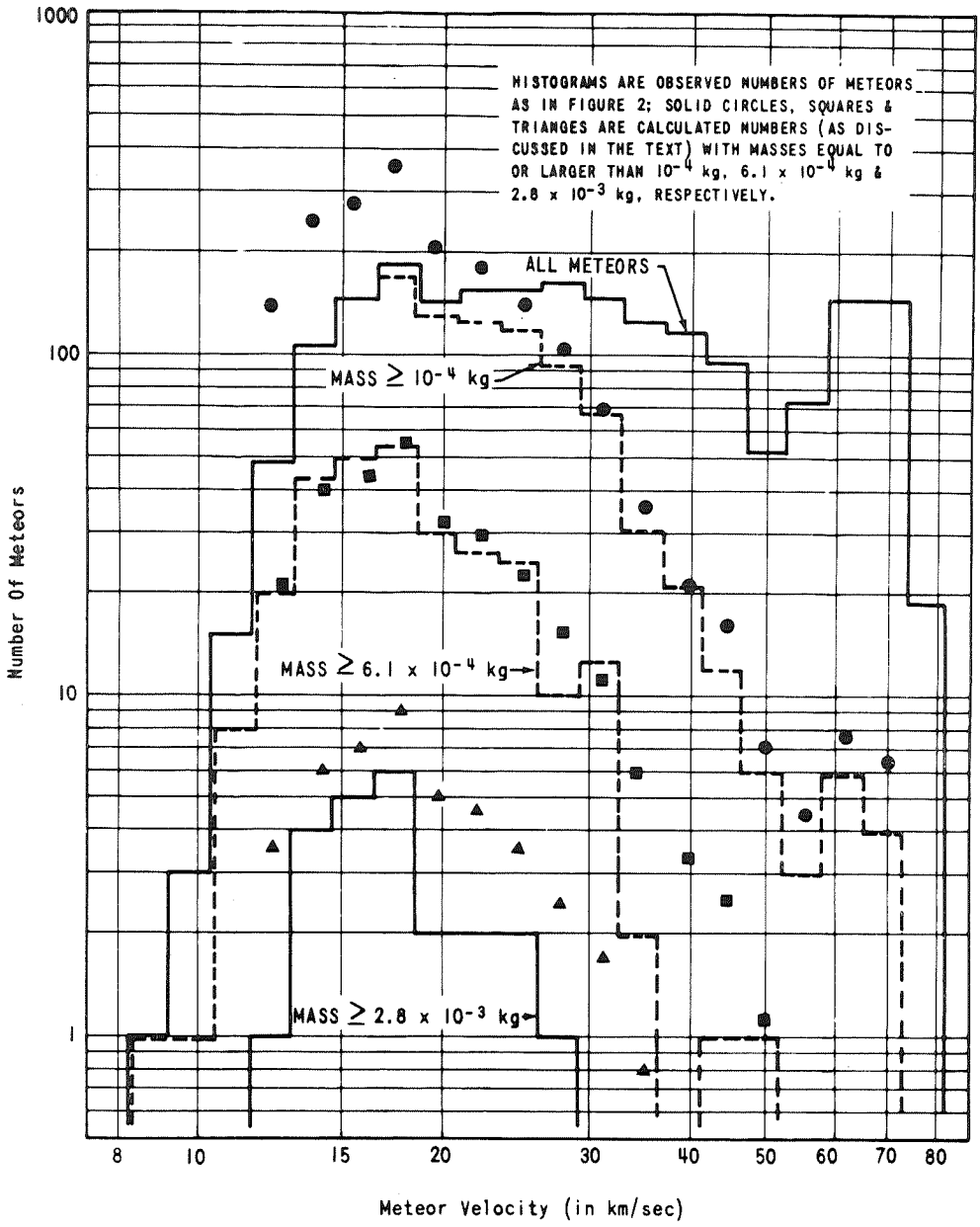
HISTOGRAMS ARE OBSERVED NUMBERS OF METEORS AS IN FIGURE 2; SOLID CIRCLES, SQUARES & TRIANGES ARE CALCULATED NUMBERS (AS DISCUSSED IN THE TEXT) WITH MASSES EQUAL TO OR LARGER THAN 10^{-4} kg, 6.1×10^{-4} kg & 2.8×10^{-3} kg, RESPECTIVELY.
ALL METEORS
MASS $\geq 10^{-4}$ kg
MASS $\geq 6.1 \times 10^{-4}$ kg
MASS $\geq 2.8 \times 10^{-3}$ kg
1000
100
10
1
Number Of Meteors
8
10
15
20
30
40
50
60
70
80
Meteor Velocity (in km/sec)

FIGURE 22

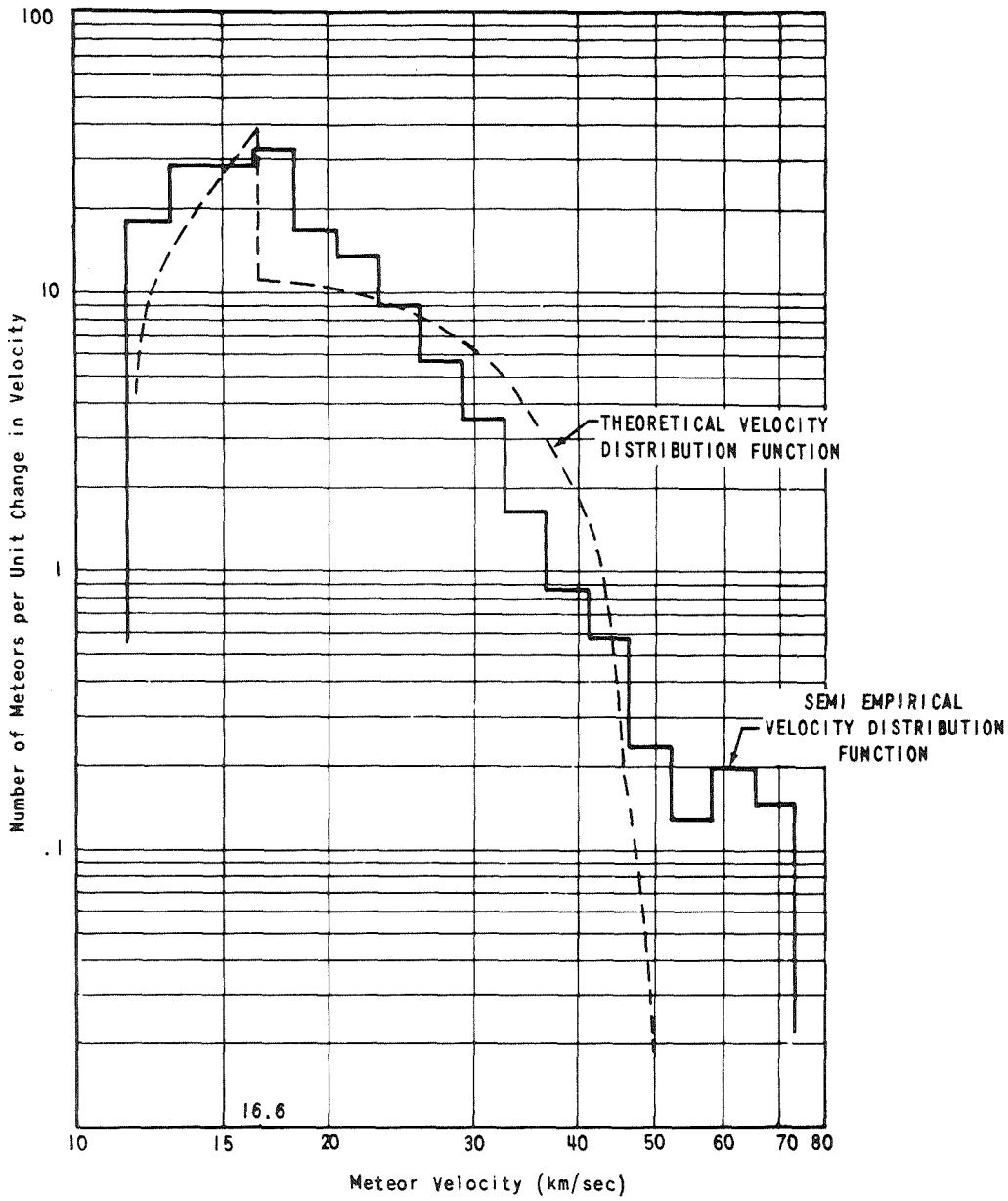
100
10
1
.1
Number of Meteors per Unit Change in Velocity
THEORETICAL VELOCITY
DISTRIBUTION FUNCTION
SEMI EMPIRICAL
VELOCITY DISTRIBUTION
FUNCTION
16.6
10
15
20
30
40
50
60
70
80
Meteor Velocity (km/sec)

FIGURE 23

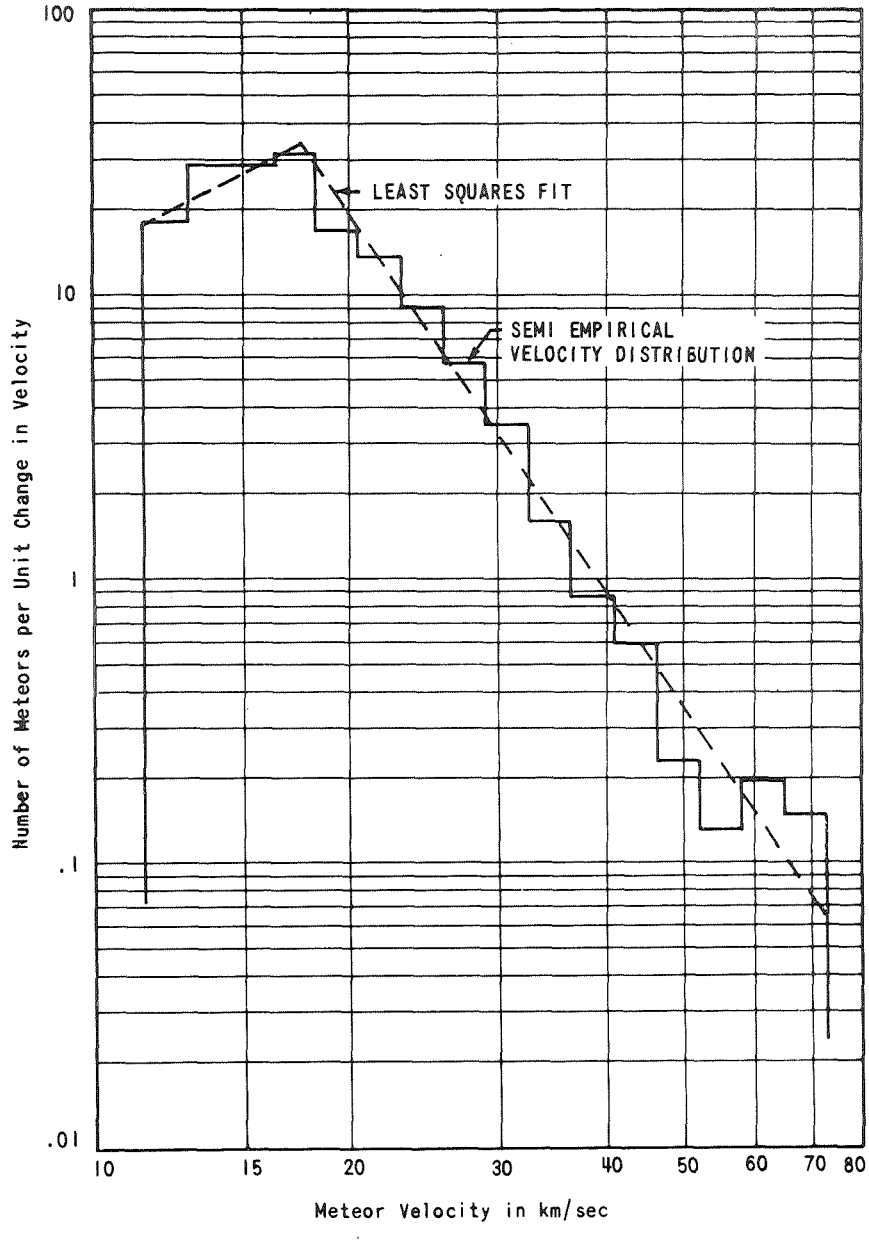
100
10
1
.1
.01
LEAST SQUARES FIT
SEMI EMPIRICAL
VELOCITY DISTRIBUTION
Number of Meteors per Unit Change in Velocity
10
15
20
30
40
50
60
70
80
Meteor Velocity in km/sec

FIGURE 24

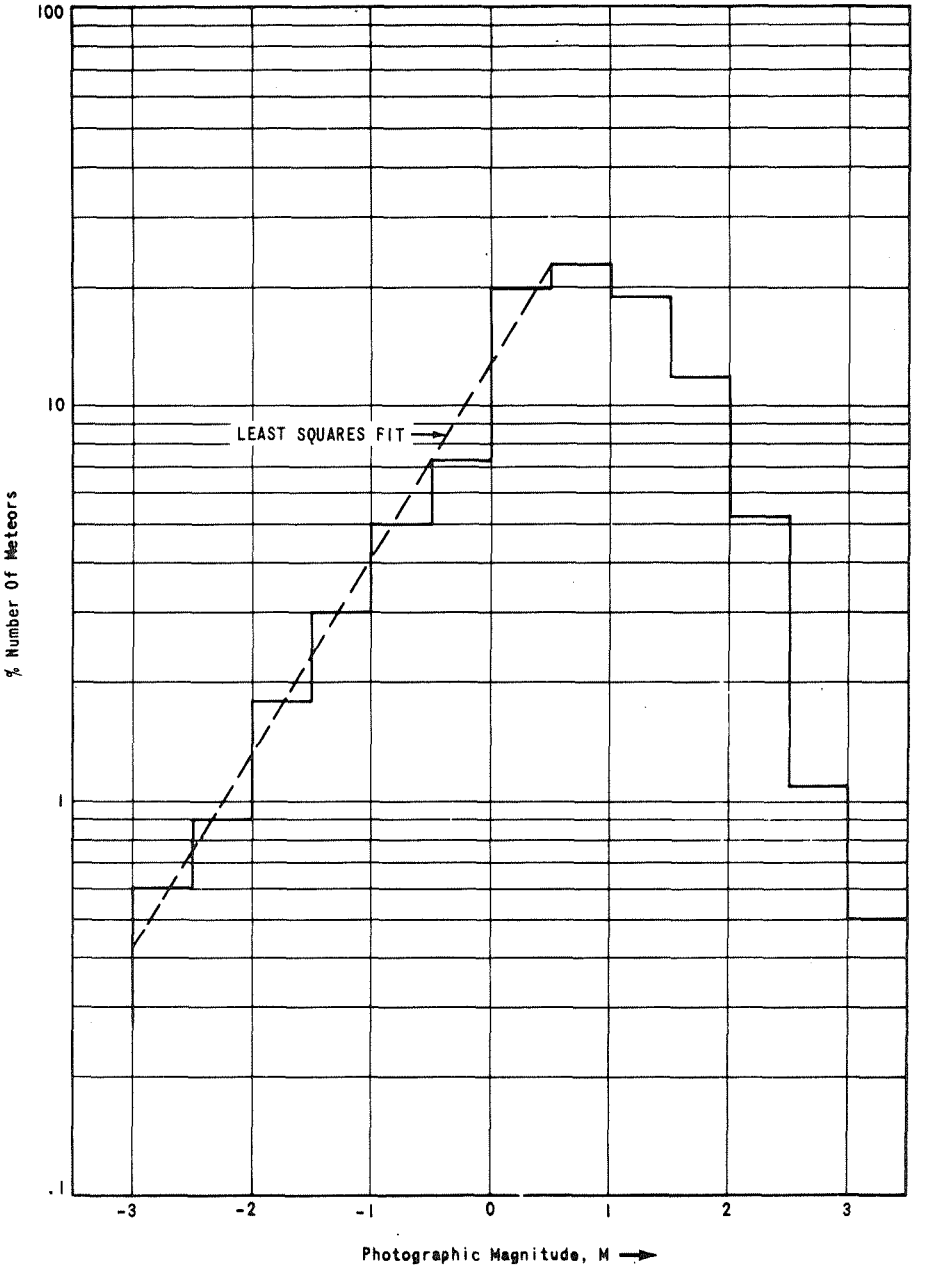
100
10
1
.1
% Number Of Meteors
LEAST SQUARES FIT
-3
-2
-1
0
1
2
3
Photographic Magnitude, M

FIGURE 25